stability and tissue disposition of the delivery system should be altered, followed by decreased potential in targeted delivery of drugs to the target.

In a series of our investigations, we have established polymeric micelles prepared from AB-type block copolymers to attain effective novel drug delivery for antitumor drugs [9–12]. A polymeric micelle in a size range <200 nm reduces non-selective reticuloendothelial system (RES) scavenge and shows enhanced permeability and retention effects (EPR effect) [13] at solid tumor sites for passive targeting. Our studies revealed that the stability of micellar structures in the presence of rabbit serum of adriamycin-conjugated poly(ethylene oxide)-poly(aspartic acid) block copolymers was largely influenced by chemical structure of block copolymers and well correlated with in vivo antitumor activity [14].

Our previous study for CPT showed that CPT incorporation efficiency and CPT-loaded micelles stability were improved by modification of a hydrophobic segment of the poly(ethylenglycol)-poly(aspartate) block copolymer as well as by choosing an appropriate incorporation method [15]. In the present study, we investigate the stability of CPT and CPT-loaded polymeric micelles in the presence of serum and serum albumins from different species (bovine, murine, and human) by reverse-phase HPLC and gel permeation chromatography. In particular, our discussion will focus on the strategy of polymeric micelles for enhanced stability of CPT.

2. Materials and methods

2.1. Materials

Poly(ethylene glycol)-poly(benzyl L-aspartate-69) block copolymer (PEG-P(Asp(Bz-69)) was synthesized by benzyl esterification of poly(ethylene glycol)-poly(aspartic acid) (PEG-P(Asp)) as described previously [15]. Composition of this block copolymer was determined by a ^{1}H NMR spectrum. The chemical structure of PEG-P(Asp(Bz)) is shown in Fig. 1b. Molecular weight of the poly(ethylene glycol) (PEG) chain was 5000 and the average number of aspartate units was 27.1. Sixty-nine percent of the aspartic acid residue was esterified with benzyl group, while the other 31% residue remained unesterified. Approximately 75% of the aspartic acid residues were of the β-amide form due to an alkaline hydrolysis procedure in this block copolymer synthesis. (s)-(+)-Camptothecin was purchased from Aldrich Chem. Co., Milw., WI, USA. Serum and albumin (fraction V) from murine (MSA), bovine (BSA), and human (HSA) were obtained from Sigma (St. Louis, MO, USA). All other chemicals were of analytical grade.

2.2. Incorporation of CPT into polymeric micelles

Incorporation of CPT into polymeric micelles was carried out by an evaporation method [16]. Briefly, a block copolymer and 10% CPT was dissolved in chloroform in a glass tube. The mixture was stirred at room temperature under nitrogen gas flow until the solvent completely evaporated. Distilled water was added, and the solution was sonicated using a probe-type sonicator (model VC 100, Sonics and Materials Inc., Connecticut, USA) in a cycle with a sonication time of 0.5 s and a standby time of 0.5 s at 80 °C for 2 min. The solution was centrifuged at 3900 rpm for 10 min. Subsequently, the supernatant was collected and filtrated through a nylon membrane filter with a 1 μm pore (Puradisc 25NYL, 6751-2510, Whatman, USA).

CPT-loaded polymeric micelles were dissolved in a mixture of DMSO:H_2O (9:1). The amount of CPT incorporated into polymeric micelles was determined by UV–vis absorption at 365 nm.

2.3. Reverse-phase HPLC analysis of lactone–carboxylate ratio of CPT

Reverse-phase HPLC system was utilized for simultaneous determination of the lactone and carboxylate form ratio of CPT [17]. A lactone form and an open carboxylated form of CPT were separated within a single chromatographic run. Reverse-phase HPLC system for this determination consisted of a JASCO HyPer LC-800 system (Tokyo, Japan) at a flow rate of 1.0 ml/min at 40 °C. For separation a Waters μBondasphere C_{18} reverse-phase column (3.9 × 150 mm, Nihon Waters, Tokyo, Japan) was used. The mobile phase was composed of 23% acetonitrile and 77% aqueous buffer (0.1 M KH_2PO_4, 0.5 mM tetrabutylammonium dihydrogen phosphate and 0.4 mM triethylamine at pH 6). The detection was performed using a fluorescence detector with an

excitation wavelength of 360 nm and emission wavelength of 430 nm.

2.4. Hydrolysis kinetics of CPT

The effects of serums and albumins on the hydrolysis kinetic of CPT were performed at 25 ± 0.5 °C in phosphate buffer solution pH 7.4 (PBS). Stock solution of drug was prepared in DMSO at 1 mg/ml. Further dilution at 10 μg/ml was made in PBS buffer pH 7.4 (control), serums (FBS and human serum), or 4% albumins (BSA, MSA and HAS) dissolved in PBS. Ten microliter aliquots of the reaction solutions were withdrawn periodically and immediately analyzed for both lactone and carboxylate forms of CPT by reverse-phase HPLC as described above.

2.5. Hydrolysis kinetics of CPT-loaded polymeric micelles

To elucidate protection effects of polymeric micelles on the lactone ring of CPT against its hydrolysis, CPT-loaded polymeric micelles were mixed with an equal volume of PBS (control), serum (FBS and human serum), or 8% albumins (BSA, MSA and HAS) dissolved in PBS. This mixture was incubated at 25 ± 0.5 °C. Ten microliter aliquots were withdrawn at time interval (0, 2, 4, 6, 8 and 24 h), dissolved in DMSO and appropriately diluted with buffer, followed by an immediate reverse-phase HPLC analysis for the lactone form and the carboxylate form of CPT as described above.

2.6. Stability of CPT-loaded polymeric micelles

The stability of drug-loaded micelles was determined by gel permeation chromatography (GPC) as described previously [18]. CPT-loaded micelles were mixed with an equal volume of PBS (control), serum (FBS and human serum), or 8% albumins (BSA, MSA and HAS) dissolved in PBS. This mixture was incubated at 25 ± 0.5 °C, and 100 μl aliquots were withdrawn at time interval (0, 2, 4, 6, 8 and 24 h), followed by immediate application to GPC analysis. High performance liquid chromatography (HPLC) was carried out using a JASCO HyPer LC-800 system (Tokyo, Japan) equipped with a Tosoh TSKgel G4000PW$_{XL}$ column at 40 °C. Samples (100 μl) were injected into the column and eluted with 0.1 M phosphate buffer solution (pH 7.4) at a flow rate of 1.0 ml/min. The detection was performed by absorption at 351 nm using a JASCO UV-870 detector.

For the pre-incubation experiment, CPT-loaded micelles were incubated with an equal volume of PBS (control), serum (FBS and human serum), or 8% albumins (BSA, MSA and HAS) for 1 h at 25 ± 0.5 °C. Then the mixture was added an equal volume of human serum. At time interval (0, 2, 4, 6, 8 and 24 h), 100 μl aliquots were withdrawn and followed by immediate application to GPC analysis as described above.

2.7. In vitro release from dialysis tube

Release of CPT from a dialysis tube was measured using a Spectra/Por®-4 dialysis membrane (12,000–14,000 MWCO, Spectrum Laboratories, USA) as previously reported [19]. A 100 ml phosphate-buffered saline (PBS) at pH 7.4 was used as a medium at 37 ± 0.1 °C under constant stirring. CPT-loaded polymeric micelles were mixed with an equal volume of PBS (control) or 8% albumins dissolved in PBS. One milliliter of these mixtures were placed in a dialysis bag and immersed in the medium. At certain time intervals, 1 ml aliquots of the medium were withdrawn, and the same volume of fresh medium was added. The sample solution was analyzed by reverse-phase HPLC. All experiments were performed in triplicate.

2.8. Data and statistical analysis

All the data are expressed as mean ± SD. The lactone form hydrolysis and CPT-loaded micelles stability were expressed as percentage to control. Comparisons were statistically using one-way analysis of variance (ANOVA), followed by Dunnett's test. A p-value <0.05 was considered statistically significant.

3. Results and discussion

As a result of preclinical trials being conducted world-wide, unexpected severe systemic toxicity and

poor tumor response were reported mainly due to rapid formation of the open ring form of CPT, which is tenfold less potent than the CPT lactone form [20]. The carboxylate form of CPT preferentially binds to human serum albumin (HSA), which further reduces the equilibrium amount of active lactone and greatly decreases antitumor efficacy [21,22]. Therefore factors influencing the lactone–carboxylate equilibrium of CPT are regarded as important determinants of the function of CPT. To increase the stability of lactone ring and efficacy of CPT in vivo, a number of drug delivery systems have been developed. However, in order to achieve highly clinically therapies, we need to pay great attention to interactions of carriers with biological components such as serum proteins.

In our series of investigations, we successfully synthesized poly(ethylene glycol)-poly(aspartate ester) block copolymers and optimized chemical structure of an inner core segment (hydrophobic) to obtain high incorporation efficiency and stable CPT-loaded micelles [15]. We found that high benzyl ester content such as benzyl 69% of the hydrophobic segment showed the highest CPT incorporation efficiency and the most stable CPT-loaded micelles [19]. The structure of this block copolymer is shown in Fig. 1b.

Fig. 2 compares CPT hydrolysis profiles at 25 ± 0.5 °C of 10 μg/ml CPT in PBS buffer pH 7.4 for the control and in the presence of purified serum albumins in PBS buffer (panel a) and in serum samples (panel b). The inverse linear relationship obtained between the logarithmic concentration of CPT lactone form and time indicates that the hydrolysis of CPT follows pseudo-first-order kinetics. The amount of lactone versus time was fitted to the equation $y=a\ \exp(-kt)$, where a is equivalent to the total concentration of lactone at $t=0$.The hydrolysis rate constants (k) and half-life of CPT are summarized in Table 1. The half-life of hydrolysis was calculated from $t_{1/2}=0.693/K$, where K represents the pseudo-first-order hydrolysis rate constant [5]. The results revealed marked differences between CPT stability in the presence of human albumin versus other species. The rapid CPT lactone ring opening was observed in the presence of human albumin whereas bovine and murine albumin provided slower CPT lactone ring opening than PBS buffer (control) as shown in Fig. 2a. There was

Table 1
Hydrolysis rate and half-life ($t_{½}$) of CPT at 25 ± 0.5 °C in the presence of serums and albumins from various species ($n=3$)

Compounds	Hydrolysis rate ($\times 10^{-3}$ min^{-1})	Half-life (min)
PBS buffer (control)	7.4	94
Bovine serum albumin (BSA)	0.8	771
Murine serum albumin (MSA)	1.7	408
Human serum albumin (HSA)	15.7	54
Fetal bovine serum (FBS)	10.8	64
Human serum (HS)	17.7	39

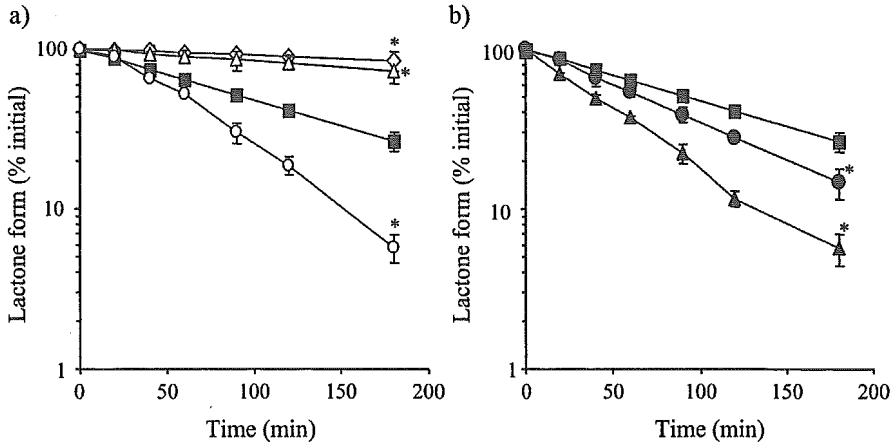

Fig. 2. Kinetic evaluation of the rate of lactone ring opening for camptothecin (CPT) evaluated by reverse-phase HPLC in the presence of albumins (panel a): (■) PBS (control); (△) 4% MSA; (◇) 4% BSA; (○) 4% HSA and whole serum (panel b): (●)FBS; (▲) human serum ($n=3$); *$p<0.05$ compared with PBS (control).

approximately 8- and 4-fold increase in the stability of CPT in the presence of BSA and MSA, respectively. This corresponded to an increase in the half-life of CPT from 94 min in PBS to 771 and 408 min in the presence of BSA and MSA, respectively. This can happen if BSA and MSA promoted the J-type self-aggregation, which was in an equilibrium with the free drug. The J-type self-aggregates were more resistant to the hydrolysis into the carboxylate form. This could be proved in the further. Self-aggregate forms of CPT were built up under certain dilution conditions of the stock DMSO solutions of CPT. They were formed by the stacking interaction between quinoline rings of CPT chromophores with the inverse position of the nitrogen atoms. This aggregation prevented hydrolysis of the lactone ring at neutral pH, thus preserving the drugs in a biologically active form [6]. Moreover, Nabiev et al. [7] reported that an addition of BSA did not induce either disaggregation or hydrolysis of the lactone ring, whereas the monomeric form of the drug was shown to undergo rapid conversion to an inactive carboxylate form in the presence of HSA. Interaction of with HSA induces disaggregation of the self-aggregate forms of CPT. On the other hand, BSA did not participate in binding of the lactone, carboxylate or self-aggregate forms of CPT [6]. Both serums (human and fetal bovine serum) showed rapid CPT lactone ring opening more than in PBS buffer (Fig. 2b). The stability of CPT incubated with HSA paralleled that of the drug in human serum. This suggests that the abundant human serum albumin protein was the major component of serum responsible for promoting rapid and extensive hydrolysis of the drug. This result was consistent with the previous reports of Mi and Burke (1994) [5]. However, an absolute value of the half-life of the hydrolysis obtained in this experiment was considerably different from the reported values in previous [5,23]. This discrepancy could be due to differences in experimental conditions such as CPT and albumin concentration, temperature, pH and so on. On the other hand, stability of CPT incubated with BSA was different from the fetal bovine serum. This result suggests that other blood components were responsible for the lactone form hydrolysis or serum reduce the self-aggregate forms of CPT. Further study is needed to elucidate these points.

As previously reported, the CPT-lactone form was preserved in the inner core of the micelles to an extent of 95% and more [15]. The micelle structure was found to greatly contribute to keep CPT in this biologically active lactone form. Therefore, in this study we focus on effects of serum and albumins in different species on the CPT-loaded micelles stability. The results showed that these CPT-loaded micelles

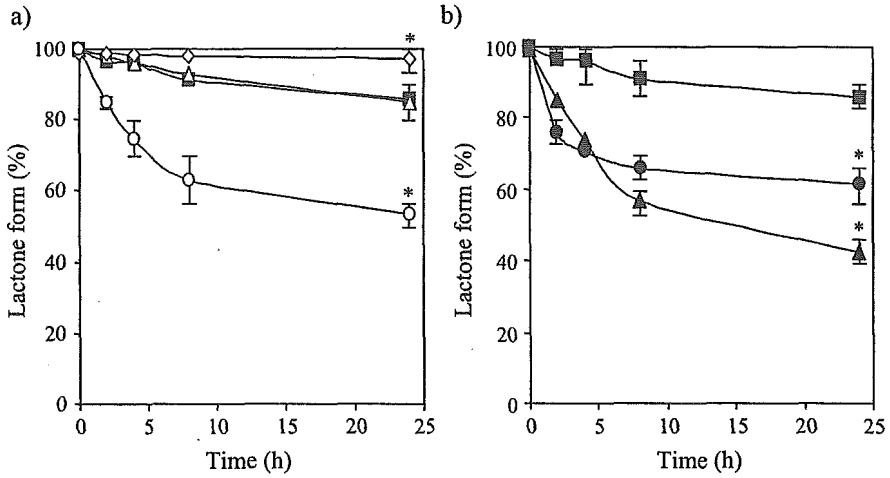

Fig. 3. Kinetic evaluation of the rate of lactone ring opening for camptothecin (CPT)-loaded polymeric micelles forming form PEG-P(Asp(Bz-69) block copolymer evaluated by reverse-phase HPLC in the presence of albumins (panel a): (■) PBS (control); (△) 4% MSA; (◇) 4% BSA; (○) 4% HSA, and serum (panel b): (●) 50% FBS; (▲) 50% human serum ($n=3$); *$p<0.05$ compared with PBS (control).

Table 2
Hydrolysis rate and half-life ($t_{1/2}$) of CPT-loaded polymeric micelles at 25 ± 0.5 °C in the presence of serums and albumins from various species (n=3)

Compounds	Hydrolysis rate ($\times 10^{-3}$ h^{-1})	Half-life (h)
PBS buffer (control)	0.6	116
Bovine serum albumin (BSA)	0.7	990
Murine serum albumin (MSA)	6.6	105
Human serum albumin (HSA)	23	30
Fetal bovine serum (FBS)	14	50
Human serum (HS)	33	21

protected lactone ring for a long time (Fig. 3). The hydrolysis of CPT lactone forms of CPT-loaded micelles follows pseudo-first-order kinetics. The hydrolysis rate constants (k) and half-life of CPT are summarized in Table 2. The half-lives of CPT lactone form in the presence of albumins (BSA, HSA, and MSA) and FBS were over 24 h except for human serum of 21 h. Fig. 3a showed that the rapid CPT lactone ring opening was observed only in the presence of human albumin whereas bovine and murine albumins retarded CPT lactone ring opening in comparison with PBS buffer (control). This result was consistent with the results obtained by GPC (Fig. 4). GPC with UV detection allowed us to evaluate the nature of the resulting particles and the degree of drug incorporation [24]. The CPT-loaded micelles peak was detected at the gel-exclusion volume at retention time of 5.2 min. The stability of CPT-loaded micelles was characterized by peak area of the peak detected by UV absorption at 351 nm. This peak area represents the amount of CPT loaded into the micelles. Therefore, a peak area was larger, CPT loaded in the micelle was more stable. The results showed that human albumin, human serum, and FBS significantly destabilized the CPT-loaded micelles while BSA showed a little increase in the micelle stability whereas, no effect for MSA in comparison with control. These results indicated that CPT-loaded micelle stabilities were responsive to albumins and serums from different species and that human albumin played a key role in destabilization of CPT-loaded micelles.

Fig. 5 shows the results of CPT-loaded micelles stability when these micelles preincubated with purified serum albumins (BSA, MSA, and HSA) for 1 h prior to the addition of human serum determined by GPC. The results also indicated that BSA and MSA enhanced the stability of CPT-loaded micelles in the presence of human serum. Whereas, HSA significantly accelerated CPT-loaded micelles destabilized in comparison with PBS as control. These differences could be explained in terms of the preferential binding of CPT free drug in the open form to HSA [25]. Fig. 6 shows CPT release from a dialysis bag for CPT-loaded micelles mixed with PBS (control), 4% BSA, and 4% HSA. In the presence of

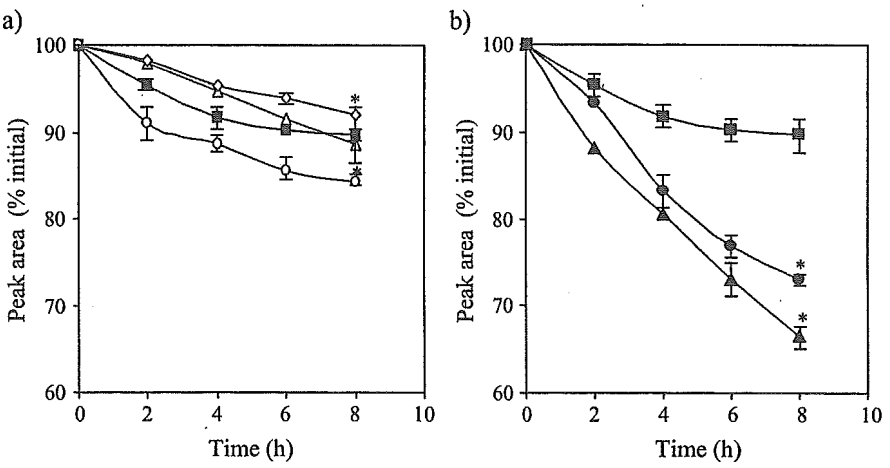

Fig. 4. Stability of camptothecin (CPT)-loaded polymeric micelles forming form PEG-P(Asp(Bz-69) block copolymer evaluated by GPC in the presence of albumins (panel a): (■) PBS (control); (△) 4% MSA; (◇) 4% BSA; (○) 4% HSA, and serum (panel b): (●) 50% FBS; (▲) 50% human serum (n=3); *p<0.05 compared with PBS (control).

BSA, CPT release from the dialysis bag was similar to the PBS (control) and providing 80% CPT release in 24 h. On the other hand, in the presence of HSA, less than 10% CPT was released in 24 h and the release rate was constant at all the investigated time. These results indicated that HSA inhibited CPT free drug release from the dialysis tube (MWCO=12,000–14,000), because only unbound CPT could pass through this tube. These differences could be explained that CPT was released from the micelles and this free drug strongly bound to HSA resulting in few CPT released through the dialysis membrane in the medium. BSA did not bind to the lactone, carboxylate, or the self-aggregate form of CPT as reported by Nabiev et al. [6], resulting in no effect for BSA on CPT release from the dialysis tube. HSA strongly binds to CPT carboxylate form and induce disaggregation of the self-aggregates of CPT, resulting in accelerated the shift of lactone to carboxylate form, finally destabilized the CPT-loaded micelles. On the other hand, the CPT incorporation stability increased in the presence of BSA, as shown in Fig. 5. This stability increase may be achieved by BSA binding to the hydrophobic inner core of the micelles. The bound BSA might work as a physical barrier for the CPT release from the micelle inner core to an aqueous medium.

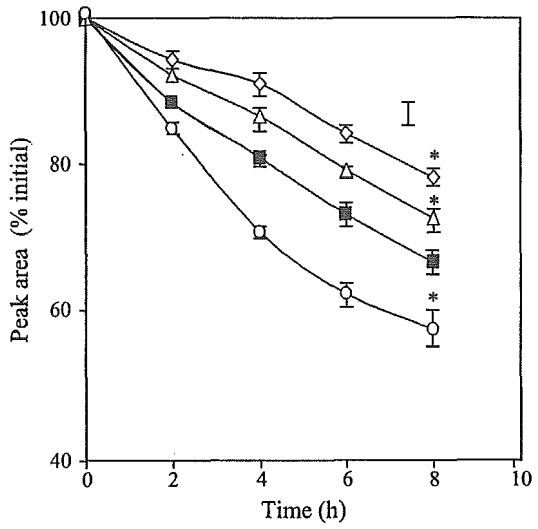

Fig. 5. Effect of pre-incubated with albumins (■ PBS (control); △ 4% MSA; ◇ 4% BSA; ○ 4% HSA) on stability of camptothecin (CPT)-loaded polymeric micelles forming form PEG-P(Asp(Bz-69) block copolymer in the presence of human serum evaluated by GPC; $*p<0.05$ compared with PBS (control).

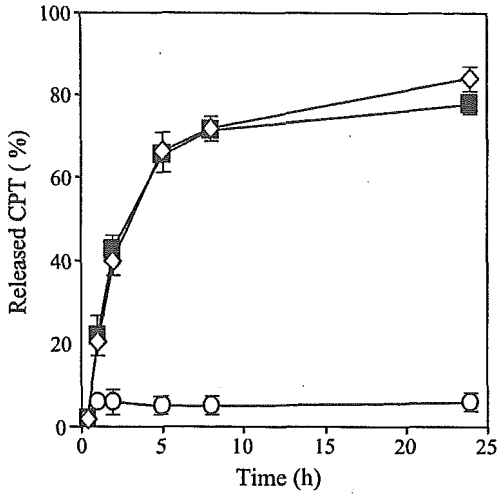

Fig. 6. Effect of pre-incubated with albumins (■ PBS (control); ◇ 4% BSA; and ○ 4% HSA) on released of CPT-loaded polymeric micelles forming form PEG-P(Asp(Bz-69) block copolymer by dialysis tube (MWCO=12,000–14,000) ($n=3$).

4. Conclusion

Polymeric micelles could preserve the CPT lactone form in the inner core of the micelles. Serum binding proteins such as albumin can bind to CPT free drug after the drug release from the inner core. HSA preferentially binds to the carboxylate form resulting in changing the lactone–carboxylate equilibrium and destabilized the micelles. On the other hand, BSA did not bind to the lactone form but might promote the self-aggregation of CPT and binding to the hydrophobic inner core of the micelles, resulting in enhanced stability of CPT-loaded micelles. MSA did not affect on the stability of micelles. This could be very important data concerning for the success in the extrapolation of both pharmacokinetic modeling and efficacy data for these agents from animal models to humans.

Acknowledgments

This work is supported by a Health and Labor Sciences Research Grant for Research on Hepatitis

and BSE from the Ministry of Health, Labor and Welfare of Japan, and a Grant-in-Aid from the Ministry of Health, Labor and Welfare of Japan. The first author acknowledges a postdoctoral fellowship for foreign researchers from Japan Society for the Promotion of Science (JSPS).

References

[1] R.P. Hertzberg, M.J. Caranfa, S.M. Hecht, On the mechanism of topoisomerase I inhibition by camptothecin: evidence for binding to an enzyme–DNA complex, Biochemistry 28 (1989) 4629–4638.

[2] J. Fassberg, V.J. Stella, A kinetic and mechanistic study of the hydrolysis of camptothecin and some analogues, J. Pharm. Sci. 81 (1992) 676–684.

[3] Z. Mi, T.G. Burke, Differential interactions of camptothecin lactone and carboxylate forms with human blood components, Biochemistry 33 (1994) 10325–10336.

[4] B.C. Giovanella, N. Harris, J. Mendoza, Z. Cao, J. Liehr, J.S. Stehlin, Dependence of anticancer activity of camptothecins on maintaining their lactone function, Ann. N. Y. Acad. Sci. 922 (2000) 27–35.

[5] Z. Mi, T.G. Burke, Marked interspecies variations concerning the interactions of camptothecin with serum albumins: a frequency-domain fluorescence spectroscopic study, Biochemistry 33 (1994) 12540–12545.

[6] F. Fleury, I. Kudelina, I. Nabiev, Interactions of lactone, carboxylate and self-aggregated forms of camptothecin with human and bovine serum albumins, FEBS Lett. 406 (1997) 151–156.

[7] I. Nabiev, F. Fleury, I. Kudelina, Y. Pommier, F. Charton, J.F. Riou, A.J. Alix, M. Manfait, Spectroscopic and biochemical characterisation of self-aggregates formed by antitumor drugs of the camptothecin family: their possible role in the unique mode of drug action, Biochem. Pharmacol. 55 (1998) 1163–1174.

[8] P. Opanasopit, M. Nishikawa, M. Hashida, Factors affecting drug and gene delivery: effects of interaction with blood components, Crit. Rev. Ther. Drug Carr. Syst. 19 (2002) 191–233.

[9] M. Yokoyama, T. Okano, Y. Sakurai, H. Ekimoto, C. Shibazaki, K. Kataoka, Toxicity and antitumor activity against solid tumors of micelle-forming polymeric anticancer drug and its extremely long circulation in blood, Cancer Res. 51 (1991) 3229–3236.

[10] M. Yokoyama, T. Okano, Y. Sakurai, S. Fukushima, K. Okamoto, K. Kataoka, Selective delivery of adriamycin to a solid tumor using a polymeric micelle carrier system, J. Drug Target. 7 (1999) 171–186.

[11] M. Yokoyama, A. Satoh, Y. Sakurai, T. Okano, Y. Matsumura, T. Kakizoe, K. Kataoka, Incorporation of water-insoluble anticancer drug into polymeric micelles and control of their particle size, J. Control. Release 55 (1998) 219–229.

[12] Y. Mizumura, Y. Matsumura, M. Yokoyama, T. Okano, T. Kawaguchi, F. Moriyasu, T. Kakizoe, Incorporation of the anticancer agent KRN5500 into polymeric micelles diminishes the pulmonary toxicity, Jpn. J. Cancer Res. 93 (2002) 1237–1243.

[13] K. Greish, J. Fang, T. Inutsuka, A. Nagamitsu, H. Maeda, Macromolecular therapeutics: advantages and prospects with special emphasis on solid tumour targeting, Clin. Pharmacokinet. 42 (2003) 1089–1105.

[14] M. Yokoyama, G.S. Kwon, T. Okano, Y. Sakurai, M. Naito, K. Kataoka, Influencing factors on in vitro micelles stability of adriamycin-block copolymer conjugates, J. Control. Release 28 (1994) 59–65.

[15] M. Yokoyama, P. Opanasopit, Y. Maitani, K. Kawano, T. Okano, Polymer design and incorporation method for polymeric micelle carrier system containing water-insoluble anti-cancer agent camptothecin, J. Drug Target. 12 (2004) 373–384.

[16] A. Lavasanifar, J. Samuel, G.S. Kwon, Micelles self-assembled from poly(ethylene oxide)-block-poly(*N*-hexyl stearate L-aspartamide) by a solvent evaporation method: effect on the solubilization and haemolytic activity of amphotericin, B. J. Control. Release 77 (2001) 155–160.

[17] A. Shenderova, T.G. Burke, S.P. Schwendeman, The acidic microclimate in poly(lactide-co-glycolide) microspheres stabilizes camptothecins, Pharm. Res. 16 (1999) 241–248.

[18] M. Yokoyama, G.S. Kwon, T. Okano, Y. Sakurai, K. Kataoka, Influenceing factors on in vitro micelle stability of adriamycin-block copolymer conjugates, J. Control. Release 28 (1994) 59–65.

[19] P. Opanasopit, M. Yokoyama, M. Watanabe, K. Kawano, Y. Maitani, T. Okano, Block copolymer design for camptothecin incorporation into polymeric micelles for passive tumor targeting, Pharm. Res. 21 (2004) 2001–2008.

[20] W.J. Slichenmyer, E.K. Rowinsky, R.C. Donehower, S.H. Kaufmann, The current status of camptothecin analogues as antitumor agents, J. Natl. Cancer Inst. 85 (1993) 271–291.

[21] Z. Mi, T.G. Burke, Differential interactions of camptothecin lactone and carboxylate forms with human blood components, Biochemistry 33 (1994) 10325–10336.

[22] I. Chourpa, J.M. Millot, G.D. Sockalingum, J.F. Riou, M. Manfait, Kinetics of lactone hydrolysis in antitumor drugs of camptothecin series as studied by fluorescence spectroscopy, Biochim. Biophys. Acta 1379 (1998) 353–366.

[23] I. Chourpa, J.M. Millot, G.D. Sockalingum, J.F. Riou, M. Manfait, Kinetics of lactone hydrolysis in antitumor drugs of camptothecin series as studied by fluorescence spectroscopy, Biochim. Biophys. Acta 1379 (1998) 353–366.

[24] M. Yokoyama, T. Sugiyama, T. Okano, Y. Sakurai, M. Naito, K. Kataoka, Analysis of micelle formation of an adriamycin-conjugated poly(ethylene glycol)-poly(aspartic acid) block copolymer by gel permeation chromatography, Pharm. Res. 10 (1993) 895–899.

[25] G.J. Finlay, B.C. Baguley, Effects of protein binding on the in vitro activity of antitumour acridine derivatives and related anticancer drugs, Cancer Chemother. Pharmacol. 45 (2000) 417–422.

Journal of
Biomedical Nanotechnology
Vol. 1, 176–184, 2005

RESEARCH ARTICLE

Folate-Linked Nanoparticles Formed with DNA Complexes in Sodium Chloride Solution Enhance Transfection Efficiency

Yoshiyuki Hattori,[1] Hajime Kubo,[2] Kunio Higashiyama,[2] and Yoshie Maitani[1,*]

[1]*Department of Fine Drug Targeting Research and* [2]*Department of Synthetic Organic Chemistry Research, Institute of Medicinal Chemistry, Hoshi University, Ebara 2-4-41, Shinagawa-ku, Tokyo, Japan 142-8501*

To enhance folate-targeted transfection efficiency, we improved folate-linked cationic nanoparticles by using cholesteryl-3β-carboxyamidoethylene-*N*-hydroxylamine (OH-Chol) as a cationic lipid and examined DNA complex (nanoplex) formation in NaCl solution. Nanoparticles (NP) were composed of OH-Chol and Tween 80, and NP-F was composed of folate–poly(ethylene glycol)–distearoylphosphatidylethanolamine conjugate (f-PEG_{2000}-DSPE) incorporated into NP. When the NP or NP-F nanoplex was formed in NaCl solution, the transfection activity in human nasopharyngeal cancer cells (KB cells) increased along with the concentration of NaCl, and NP-F formed a larger nanoplex and showed stronger transfection activity than NP. Confocal and flow cytometric analysis demonstrated that the nanoplexes formed in 50 mM NaCl solution extensively enhanced cellular uptake. Furthermore, the NP-F nanoplex formed in 50 mM NaCl solution could dissociate DNA better than the NP nanoplex. The NP-F nanoplex formed in 50 mM NaCl solution showed 6.6- and 18.9-fold enhancement of transfection activity with specific receptor association with KB cells, relative to NP-F formed in water at a charge ratio (+/−) of 1/1 and 3/1, respectively. The results of the experiments have provided optimal conditions to form folate-linked nanoparticle complexes with DNA for folate-targeted gene delivery.

Keywords: Cationic Nanoparticles, Folic Acid, Gene Delivery, Transfection, OH-Chol, Folate-Targeted, Nanoplex, NaCl.

1. INTRODUCTION

Gene delivery has become an increasingly important strategy for treating a variety of human diseases, including cancer.[1] A major focus in developing vectors for gene therapy has been tissue-specific targeting for improved safety. For targeted delivery to tumors, the cellular target often consists of a membrane-bound tumor-associated antigen. The receptor for the vitamin folic acid has been identified as a marker for ovarian carcinomas[2] and has also been found to be frequently overexpressed in a wide range of tumors;[3–5] therefore, it presents an attractive target for tumor-selective delivery. Folic acid retains its receptor-binding and endocytosing properties when covalently linked to a variety of molecules. Therefore, liposomes conjugated to a folate ligand *via* a PEG-spacer have been used for the delivery of chemotherapeutic agents and DNA to receptor-bearing tumor cells, e.g., a human nasopharyngeal cancer cell line, KB.[6–8]

Many different cationic lipids have been synthesized and shown activity in delivering genes into cells both *in vitro* and *in vivo*. A liposome formulation containing cationic cholesterol, 3-[*N*-(*N*′,*N*′-dimethylaminoethane) carbamoyl]cholesterol (DC-Chol), has been administered to patients in clinical trials for treating cancer because of its high transfection activity and low toxicity.[9] Recently, cationic cholesterol derivatives were reported among which cholesteryl-3β-carboxyamidoethylene-*N*-hydroxylamine (OH-Chol), having a hydroxy ethyl group at the amino terminal, showed the highest transfection efficiency.[10] The reason for the high transfection efficiency of liposomes with OH-Chol is the instability of the

*Author to whom correspondence should be addressed.

1550-7033/2005/1/176/009/$17.00+.25 doi:10.1166/jbn.2005.019

liposome/DNA complex (lipoplex) in endosomes, resulting in a more efficient translocation of DNA into the nucleus. Cholesteryl carboxyamido derivatives such as OH-Chol may be more effective in the transfection of DNA than cholesterol ester derivatives such as DC-Chol.

Large particle/DNA complexes show, in general, higher *in vitro* transfection efficiency than small complexes.[11,12] The size of the complex appears to determine transfection efficiency by controlling the size of the intracellular endosomal vesicles containing the complex, which affects the efficiency of DNA release into the cytoplasm.[11] The size of a lipoplex and polymer/DNA complex (polyplex) can be controlled by forming the complex in NaCl, $NaHCO_3$, or Na_2HPO_4 solution.[12–14] Recently, Zaric et al. reported that polyethyleneimine (PEI)/DNA or glucose-grafted PEI/DNA polyplexes formed in NaCl solution led to a higher transfection efficacy into human endothelial cells.[14] The best transfection conditions were obtained with large particles (1 μm) made in NaCl solution.

Previously, we reported that DC-Chol-based, folate-linked cationic nanoparticles could deliver DNA with selectively high transfection efficiency into KB cells and xenografts *via* folate receptor (FR)[15] and showed strong transfection activity in human prostate cancer LNCaP cells.[15,16] However, the folate-linked nanoparticle was tumor specific but had less transfection efficiency than a commercially available transfection reagent. In this study, we developed folate-linked nanoparticles composed of OH-Chol, which formed a large nanoparticle/DNA complex (nanoplex) in NaCl solution and enhanced the DNA transfection efficiency.

2. MATERIALS AND METHODS

2.1. Preparation of Plasmid DNA and Oligonucleotide

Plasmid DNA (about 6740 bp) encoding the luciferase marker gene under the control of the CMV promoter (pCMV-Luc) was supplied by Dr. Tanaka at the Mt. Sinai School of Medicine (NY, USA). A protein-free preparation of these plasmids was purified following alkaline lysis using maxiprep columns (Qiagen, Hilden, Germany). FITC-labeled randomized oligodeoxynucleotide (FITC-ODN) was synthesized as previously described.[15]

2.2. Preparation and Size of Nanoparticles and Nanoplexes

The synthesis of OH-Chol was done as previously described.[17] Cholesteryl-3β-carboxylic acid was condensed with *N*-hydroxyethylethylenediamine by carbonyldiimidazole in CH_2Cl_2 under a nitrogen atmosphere overnight and the residue was recrystallized from ethylacetate. Poly(ethylene glycol)–distearoylphoshatidylethanolamine (PEG_{2000}-DSPE) (mean MW of PEG: 2 kDa) and Tween 80 were obtained from NOF Co., Ltd. (Tokyo, Japan). Folate-PEG_{2000}-DSPE (f-PEG_{2000}-DSPE) was synthesized as previously reported.[16] All formulations of the nanoparticles consisted of 1 mg/ml OH-Chol as a cationic lipid, and 5 mol% Tween 80. The nanoparticle formulae listed in Table I were prepared with lipids (OH-Chol, Tween 80, PEG_{2000}-DSPE, or f-PEG_{2000}-DSPE) in 10 ml of water by the modified ethanol injection method.[16] In 1,1′-dioctadecyl-3,3,3′,3′-tetramethylindocarbocyanine perchlorate (DiI)-labeled nanoparticles, DiI (Lambda Probes & Diagnostics, Graz, Austria) was incorporated at 0.04 mol% of the total lipid. For specific applications, lyophilized NP was prepared as follows: the NP suspension was lyophilized by freezing at −80 °C, dried under vacuum in a freeze-drier (FDU-540, Tokyorikakikai, Co., LTD., Tokyo, Japan), and rehydrated at the same concentration with water before being freeze-dried.

The nanoplexes at a charge ratio (+/−) of 1/1 for co-incubation of folic acid in medium or 3/1 were formed by addition of each nanoparticle to 2 μg of DNA diluted in 50 μl of water or NaCl solution. This transfection solution was allowed to stand for 10 min at room temperature before being added to the cells. Lipofectamine 2000 (Invitrogen Corp., Carlsbad, CA) lipoplex at a charge ratio (+/−) of 2/1 of cationic lipid to DNA was prepared according to the manufacturer's protocol.

The particle size distributions were measured by the dynamic light scattering method (ELS-800, Otsuka Electronics Co., Ltd., Osaka, Japan), 10 min after the formation of the nanoplex at 25 °C, following dilution of the dispersion to an appropriate volume with water.

Table I. Formulae of FR-targeted nanoparticles and particle size of nanoparticles and nanoplexes formed in water.[a]

	Mol (%)					
Formulation	OH-Chol	Tween 80	f-PEG_{2000}-DSPE (F)	PEG_{2000}-DSPE (P)	Nanoparticle size (nm)	Nanoplex size (nm)
NP	95	5	—	—	129.9±12.0	279.1±26.4
NP-1P	94	5	—	1	167.2±5.4	241.1±3.4
NP-1F (NP-F)	94	5	1	—	180.3±6.0	319.9±7.6
NP-2F	93	5	2	—	144.7±3.8	284.8±5.9
NP-5F	90	5	5	—	229.6±14.0	212.2±1.3

All formulations consisted of 1 mg/ml OH-Chol as a cationic lipid and 5 mol% Tween 80 (NP). NP-1P consisted of NP with 1 mol% PEG_{2000}-DSPE. For FR-targeted vectors, NP-1F, -2F and -5F consisted of NP with 1, 2 and 5 mol% f-PEG_{2000}-DSPE, respectively. Nanoparticles were prepared with lipids (e.g., NP-IF, OH-Chol/Tween 80/f-PEG_{2000}-DSPE = 94/5/1, molar ratio = 10:1.3:0.65, weight (mg)) in 10 ml water by the modified ethanol injection method. [a]Charge ratio (+/−) of nanoparticle/DNA = 3/1. Values represent means ± SD ($n = 3$).

2.3. Gel Retardation Assay

One microgram of plasmid DNA was mixed with aliquots of nanoparticles (1–5 charge equivalent of nanoparticles). After a 10-min incubation of the nanoplexes in water, they were analyzed by 1.5% agarose gel electrophoresis in Tris-Borate-EDTA (TBE) buffer and visualized by ethidium bromide staining.

2.4. Cell Culture

LNCaP cells were supplied by the Department of Urology, Keio University Hospital (Tokyo, Japan). KB cells were from the Cell Resource Center for Biomedical Research, Tohoku University (Miyagi, Japan). A human cervix carcinoma cell line, Hela, was kindly provided by Toyobo Co., LTD. (Osaka, Japan). All the cell lines used in this study were grown in a folate-deficient RPMI-1640 medium (Life Technologies, Inc., Grand Island, NY) supplemented with 10% heat-inactivated fetal bovine serum (Life Technologies, Inc.) and kanamycin (100 μg/ml) at 37 °C in a 5% CO_2 humidified atmosphere.

2.5. Luciferase Assay

Based on a preliminary experiment of luciferase assay, the optimized ratio of cationic lipid to DNA was determined as 3:1. For transfection, each nanoplex was diluted in 1 ml of medium supplemented with 10% serum and then incubated for 24 h. Cells were incubated with the nanoplex in the presence or absence of 1 mM folic acid. Luciferase expression was measured using the luciferase assay system (Pica gene, Tokyo Ink Mfg. Co. Ltd., Tokyo, Japan) as previously reported.[16]

2.6. Flow Cytometric Analysis

KB cell cultures were prepared by plating the cells in a 35-mm culture dish 24 h prior to each experiment. In the DiI-labeled nanoplex, DiI-labeled nanoparticles were mixed with 2 μg of plasmid DNA in water or 50 mM NaCl at a charge ratio (+/−) of 3/1. In the FITC-labeled nanoplex for co-incubation of folic acid in medium, nanoparticles were mixed with 2 μg of FITC-ODN in water or 50 mM NaCl at a charge ratio (+/−) of 1/1. In the FITC-labeled nanoplex for cellular association, nanoparticles were mixed with 2 μg of FITC-ODN in water or 50 mM NaCl at a charge ratio (+/−) of 3/1. Then the nanoplexes were diluted in 1 ml of RPMI medium containing 10% serum and added to the monolayers of the cells. Cells were incubated with the nanoplex with 10% serum in the presence or absence of 1 mM folic acid. After 3 or 24 h incubation, the dish was washed 2 times with 1 ml of PBS (pH 7.4) to remove any unbound nanoplex, and the cells were detached with 0.05% trypsin. The amount of FITC-ODN or DiI-labeled nanoparticles in the cells was determined by examining fluorescence intensity on a FACSCalibur flow cytometer (Becton Dickinson, San Jose, CA) as previously described.[15]

2.7. Confocal Microscopy

LNCaP, KB, and Hela cells, respectively, were plated into 35-mm culture dishes. Ten microliters of each nanoparticle was mixed and incubated with 2 μg of FITC-ODN in water or 50 mM NaCl for 10 min and then diluted in 1 ml of medium supplemented with 10% serum. These cells were incubated with the nanoplex for 3 h. After incubation, cells were washed twice with PBS and fixed with 10% formaldehyde in PBS for 15 min at room temperature. For staining the nucleus, the fixed cells were washed and incubated with 0.5 mg/ml RNase in PBS for 10 min at 37 °C. Subsequently, the cells were washed and incubated with propidium iodide (PI) for 10 min at room temperature. Examinations were performed with a Radiance 2100 confocal laser scanning microscope (BioRad, CA) as previously described.[16] For PI, maximal excitation was performed with a 543-nm internal He–Ne laser, and fluorescence emission was observed with a long pass barrier filter, 560DCLP. FITC-ODN was imaged using an argon laser at 488-nm excitation, and fluorescence emission was observed with a filter, HQ515/30.

2.8. DNA Association Assay

The fluorescent intensity (FI) of FITC-ODN is increased when FITC-ODN associates with nanoparticles. To measure the amount of DNA associated with nanoparticles, 10 μl of nanoparticles and 2 μg of FITC-ODN were mixed in 50 μl of water or 50 mM NaCl and stood for 10 min at room temperature. Then FITC-ODN and its nanoplexes, respectively, were diluted with 1 ml of 0.2 M sodium phosphate buffer pH 6 or 7 and FI values (nanoplex or FITC-ODN at 0 h) were measured with a fluorometer (ex. 488 nm, em. 525 nm). After a 1-h incubation of FITC-ODN and its nanoplexes at 37 °C, both FI values (nanoplex or FITC-ODN at 1 h) were again measured and the amount of dissociated DNA was calculated as indicated below.

$$\text{Dissociated DNA (\%) at pH 6 or 7} = \left(1 - \frac{(\text{FI of nanoplex at 1 h}) - (\text{FI of FITC-ODN at 1 h})}{(\text{FI of nanoplex at 0 h}) - (\text{FI of FITC-ODN at 0 h})}\right) \times 100$$

Statistical analysis: Data were compared using analysis of variance and evaluated by Student's t test or Welch's t test. A p value of 0.05 or less was considered significant.

3. RESULTS

3.1. Formulation and Size of Nanoparticles and Nanoplexes

Five different cationic nanoparticle formulations were prepared as potential nonviral vectors. The components and compositions of the nanoparticles are presented in Table I.

All formulations consisted of 1 mg/ml OH-Chol as a cationic lipid and 5 mol% Tween 80 (NP). NP-1P consisted of NP with 1 mol% PEG_{2000}-DSPE. For FR-targeted vectors, NP-1F, -2F, and -5F consisted of NP with 1, 2, and 5 mol% f-PEG_{2000}-DSPE, respectively. The average size of each nanoparticle was 100–200 nm (Table I). When the nanoparticles were mixed with DNA at a charge ratio (+/−) of 3/1, the size of each nanoplex, except for NP-5F, increased from 250 to 300 nm.

3.2. Gel Retardation Assay

The association of plasmid DNA with each nanoparticle was monitored by gel retardation electrophoresis (Fig. 1). The migration pattern of plasmid DNA in the nanoplex changed when the plasmid DNA was mixed with nanoparticles at charge ratios (+/−) from 1 to 5 in water. The migration of plasmid DNA in the nanoplex gradually ceased as the charge ratio was increased. Beyond a charge ratio (+/−) of 3/1 in NP and NP-1F, no migration was observed. Among the nanoparticles, the disappearance of migration with increasing charge ratio (+/−) gradually was observed as the amount of f-PEG_{2000}-DSPE in nanoparticles was increased. This result indicated that the association of plasmid DNA with nanoparticles was inhibited more as the f-PEG_{2000}-DSPE content of the nanoparticle increased.

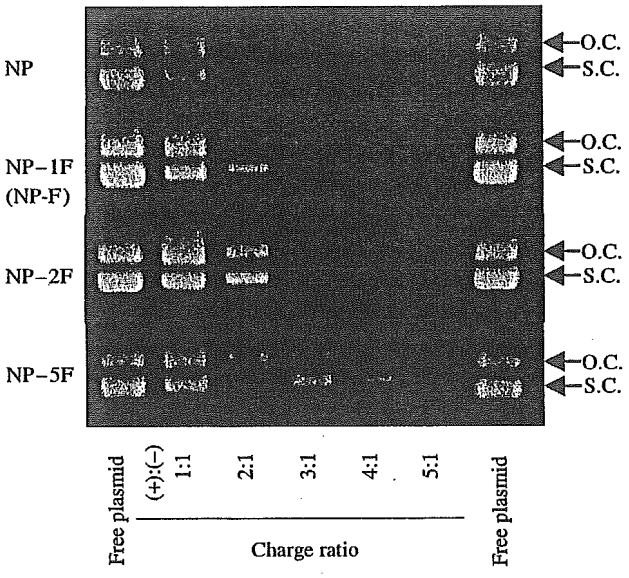

Fig. 1. Association of plasmid DNA with nanoplexes formed in water at various charge ratios (+/−) analyzed using agarose gel electrophoresis. One microgram of plasmid DNA was mixed with aliquots of nanoparticles at various charge ratios in water. After a 10-min incubation, the nanoplexes were analyzed by 1.5% agarose gel electrophoresis. Charge ratios (+/−) of nanoparticle:plasmid DNA = 1:1, 2:1, 3:1, 4:1, and 5:1. O.C. indicates open circular plasmid; S.C. indicates supercoiled plasmid.

3.3. Association of FITC-Labeled Nanoplexes Formed in Water with KB Cells

We examined the selectivity of FR-targeted nanoparticles to carry genes into KB cells using FITC-labeled nanoplexes by flow cytometry. It is reported that a negatively charged folic acid forms a charge-mediated complex with positively charged particles through its carboxyl groups and has an effect on the transfection efficiency.[18] In our nanoparticles, the nanoplexes formed at a charge ratio (+/−) of 3/1 showed a positive ζ-potential (about 30–40 mV) (data not shown). To protect to form complex of the positively charged nanoparticles with folic acid in medium, we prepared neutrally charged nanoplexes in water at a charge ratio (+/−) of 1/1 and then incubated them with KB cells for 3 h in the absence or presence of 1 mM folic acid in the medium. The presence of free folic acid in the medium significantly reduced the association with the nanoplex of NP-1F, -2F, and -5F, respectively, but not that of NP (Fig. 2). These results clearly indicated that the cellular association of FR-targeted NP occurred *via* FR.

3.4. Luciferase Expression and Association of DiI-Labeled Nanoplexes Formed in Water with KB Cells

We evaluated the transfection efficiencies of nanoparticles in KB cells at a charge ratio (+/−) of 3/1 by assaying luciferase activity. NP exhibited the highest level

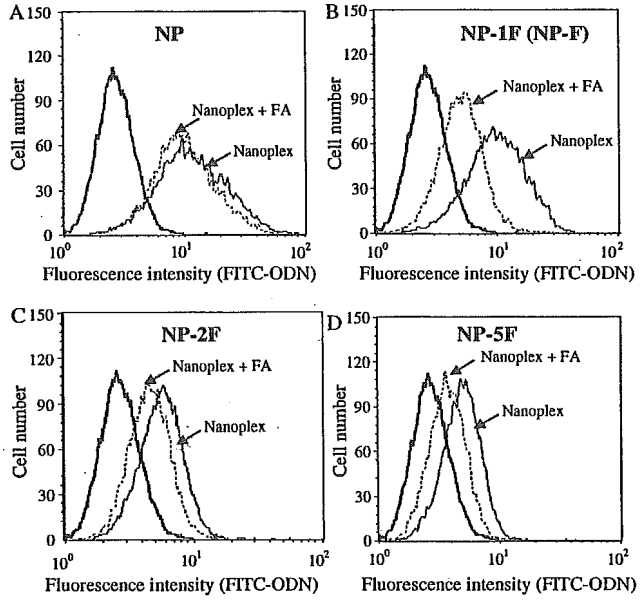

Fig. 2. Association of FITC-labeled nanoplex formed in water with KB cells 3 h after transfection in the absence or presence of free folic acid. Each nanoparticle was mixed with 2 μg of FITC-ODN at a charge ratio (+/−) of 1/1. The association was determined based on FITC-fluorescence by flow cytometry, as described in MATERIALS AND METHODS. Flow cytometry of cells exposed to the nanoplex (continuous line). Dotted line, plus 1 mM folic acid (FA); bold line, autofluorescence of the cells.

RESEARCH ARTICLE

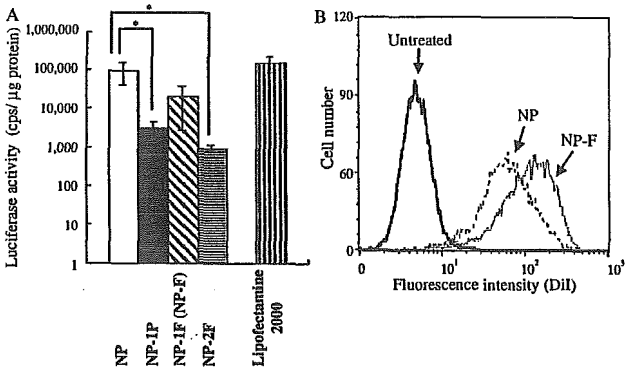

Fig. 3. Luciferase activity in KB cells transfected with various nanoplexes formed in water or lipofectamine 2000/DNA complex (A) and association of DiI-labeled nanoplexes 24 h after transfection into KB cells (B). Each nanoparticle (A) or DiI-labeled NP and NP-F (B) was mixed with 2 μg of plasmid DNA at a charge ratio (+/−) of 3/1. Each column represents the mean ± SD ($n = 3$). Statistical significance of the data was evaluated by the Student's t test. $^*P < 0.05$, compared with NP. The associations were determined based on DiI fluorescences by flow cytometry, as described in MATERIALS AND METHODS. Continuous line, NP; dotted line, NP-F; bold line, autofluorescence of the cells.

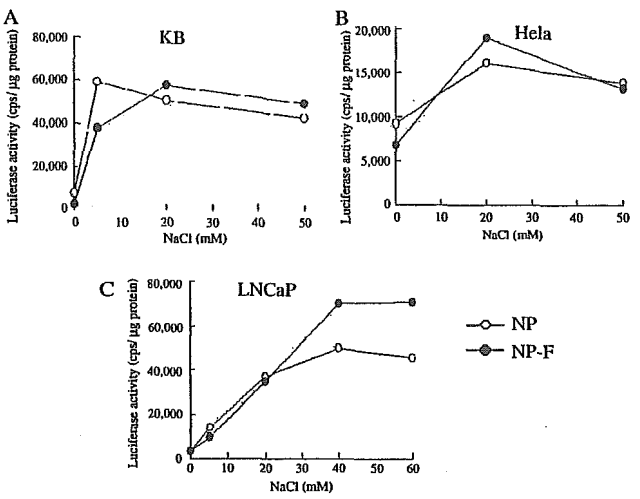

Fig. 4. Effect of concentration of sodium chloride during the formation of nanoplexes on transfection into KB (A), Hela (B), and LNCaP (C) cells. Nanoplexes were prepared by mixing DNA with nanoparticles *in various concentrations of* NaCl at a charge ratio (+/−) of 3/1. The luciferase assay was carried out 24 h after incubation of the nanoplexes. Data points indicate means ($n = 2$).

of luciferase activity among the nanoparticles (Fig. 3A). NP-1P showed 30-fold lower luciferase activity than NP, possibly due to addition of PEG_{2000}-DSPE. However, NP-1F showed 6.6-fold higher luciferase activity than NP-1P. Among the FR-targeted nanoparticles, a reduction in luciferase activity was observed as the amount of f-PEG_{2000}-DSPE added was increased. In comparison with Lipofectamine 2000, a commercial gene transfection reagent, NP showed comparable transfection activity, but NP-1F and -2F showed about 7.6- and 49.9-fold less transfection activity, respectively. In subsequent experiments, therefore, we selected NP-1F for the folate-targeted vector, referred to as NP-F.

Next, to examine the association of nanoparticles with KB cells, DiI(a nonexchangeable fluorescent membrane probe)-labeled nanoplexes were prepared from DiI-labeled nanoparticles and incubated with KB cells for 24 h. The association of NP-F nanoplex with KB cells was compared with that of NP nanoplex by flow cytometry. As shown in Figure 3B, the amount of NP-F nanoplex associated with the cells was markedly increased, compared with that of NP nanoplex, indicating that the association of NP-F nanoplex with the cell could be enhanced by folic acid linked to the nanoparticle but could not induce enough gene expression.

3.5. Effect of Nanoplex Formed in Sodium Chloride on Transfection Efficiency

The lipoplex and polyplex produced in sodium chloride were large and achieved efficient transfection.[14,19] To increase the size of the NP-F nanoplex, we prepared nanoplex formed in various concentrations of NaCl and then examined the transfection efficiency in KB, Hela, and LNCaP cells, which overexpressed folate-binding proteins.[15] The transfection activity of both NP and NP-F increased, together with the concentration of NaCl, and seemed to be saturated near 50 mM NaCl in all the cell lines (Fig. 4A–C). NP-F showed greater transfection activity than NP in KB and LNCaP cells when the nanoplexes were formed in 20 mM or more of NaCl.

3.6. Size and Cellular Association of Nanoplex in the Presence of Sodium Chloride

To clarify the effect on transfection efficiency of the nanoplex formed in water or 50 mM NaCl, we examined the change in the size of the nanoplex by dynamic light scattering and the cellular association of nanoplex by flow cytometric analysis. The size of the NP and NP-F nanoplexes was unchanged in the 300- and 400-nm diameter ranges, respectively, when mixed in water for 1 h (Fig. 5). In contrast, when mixed in 50 mM NaCl for 1 h, the size of NP and NP-F nanoplexes increased to about 400 and 800 nm, respectively. The associated amount of FITC-ODN in the NP and NP-F nanoplexes with KB cells was increased when the nanoplexes were formed in 50 mM NaCl (Fig. 6A, B). These findings seemed to correspond to the high DNA transfection efficiency (Fig. 4A).

Furthermore, to examine the effect of the size of the nanoplex on transfection efficiency, we prepared large nanoparticles (lyophilized NP) by lyophilizing and rehydrating the NP suspension and mixed with it DNA at a charge ratio (+/−) of 3/1 in water or in 50 mM NaCl. The lyophilized NP nanoplex formed in water was increased in size from about 280 to 540 nm and showed about 3-fold more luciferase expression than unlyophilized NP nanoplex 24 h after its transfer to Hela cells. Furthermore,

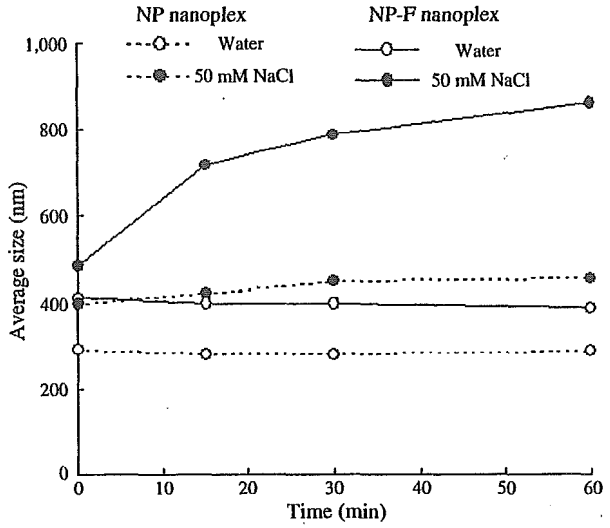

Fig. 5. Effect of sodium chloride during formation of NP and NP-F nanoplexes on their size. NP or NP-F was mixed with 2 μg of plasmid DNA in water or 50 mM NaCl at a charge ratio (+/−) of 3/1. This transfection solution was kept for 1 h at room temperature. The size distribution was determined for nanoplexes diluted with water by dynamic light scattering.

the lyophilized NP nanoplex formed in the 50 mM NaCl solution increased in size from about 540 to 810 nm and the transfection efficiency was about 1.5-fold more than that of lyophilized NP nanoplex formed in water (data not shown). These findings suggested that the large nanoplex had increased transfection efficiency.

3.7. Transfection Efficiency Visualized by Confocal Microscopy

We examined the localization of FITC-ODN after transfection into Hela and LNCaP cells by confocal microscopy. The distribution of FITC-ODN was observed in the cytoplasm weakly when NP or NP-F nanoplex was formed in water (Fig. 7A, C, E) but strongly in the cytoplasm and around the nucleus when formed in 50 mM NaCl

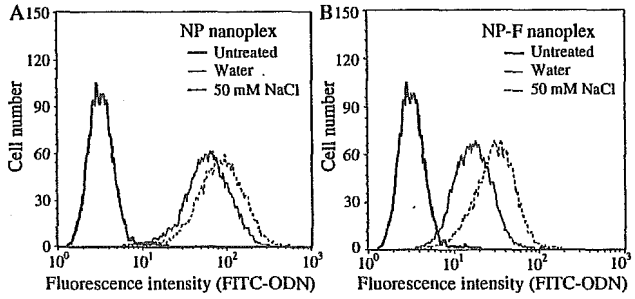

Fig. 6. Association of NP (A) and NP-F (B) nanoplexes with KB cells 3 h after transfection. In (A) and (B), nanoparticles were mixed with 2 μg of FITC-ODN in water or 50 mM NaCl at a charge ratio (+/−) of 3/1. The associations were determined based on FITC-fluorescence by flow cytometry, as described in MATERIALS AND METHODS. Continuous line, nanoplex formed in water; dotted line, in 50 mM NaCl; bold line, autofluorescence of the cells.

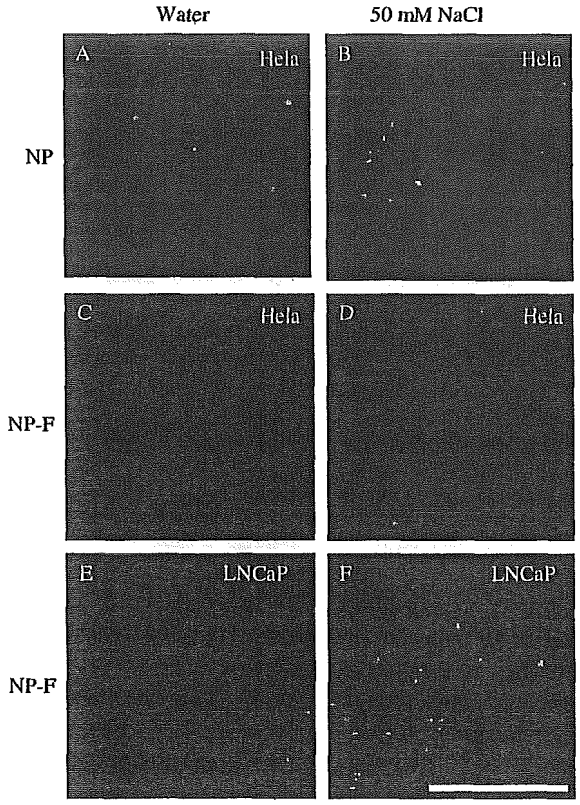

Fig. 7. Uptake of FITC-ODN transfected with NP nanoplexes (A and B) and NP-F nanoplexes (C–F) into Hela (A–D) and LNCaP (E and F) cells. Nanoplexes were prepared by mixing nanoparticles with FITC-ODN in water (A, C, and E) or 50 mM NaCl (B, D, and F) at a charge ratio (+/−) of 3/1 and then incubated with the cells for 3 h. The FITC-ODN was visualized by confocal microscopy (magnification × 600). The red signals show the localization of the nucleus, and the green signals show that of FITC-ODN. Scale bar = 50 μm.

(Fig. 7B, D, F), corresponding to the results of the FACS analysis (Fig. 6). These findings, shown in Figure 7, were also observed in KB cells (data not shown).

3.8. Dissociation of DNA from Nanoplex

To gain a further understanding of the enhancement of transfection efficiency when the nanoplex was formed in NaCl solution, we performed an assay of the association between nanoparticles and DNA in buffer of pH 6 or 7. When NP nanoplex was formed in water or 50 mM NaCl, about 15% and 10% dissociation of total DNA from NP nanoplexes was observed at pH 7, and about 25 and 30% dissociation was observed at pH 6 (Fig. 8). When NP-F nanoplex was formed in water, 10% dissociation of DNA from NP-F nanoplex was observed at pH 6 and 7. However, when NP-F nanoplex was formed in NaCl solution, about 30% and 20% of the DNA dissociated at pH 6 and 7, respectively. This finding suggests that the formation of the nanoplex in NaCl solution influenced not only the size of the nanoplex but also the dissociation of DNA from the nanoplex.

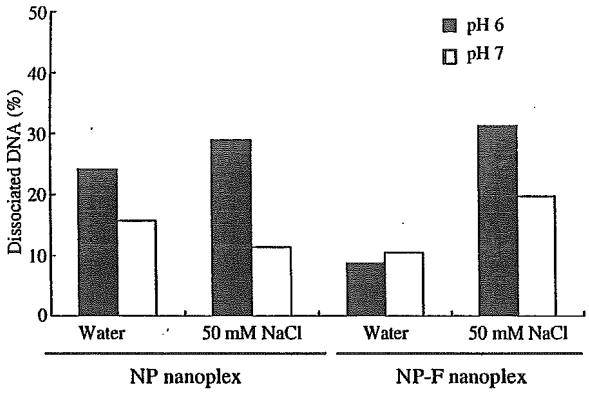

Fig. 8. Dissociation of DNA from NP or NP-F nanoplexes in the sodium phosphate buffer at pH 6 and 7. NP or NP-F was mixed with 2 μg of FITC-ODN in water or 50 mM NaCl at a charge ratio (+/−) of 3/1. The nanoplexes were incubated with sodium phosphate buffer pH 6 or 7 for 1 h, separately. The amount of dissociated DNA was calculated as described in MATERIALS AND METHODS. Data points indicate means ($n = 2$).

3.9. Transfection Efficiency of Nanoplexes Formed in NaCl in the Presence of Folic Acid

Finally, we examined the selectivity of NP-F nanoplex formed in 50 mM NaCl solution using KB cells. As shown in Figure 9, a comparative experiment in the presence of 1 mM folic acid showed that the luciferase activity of NP-F nanoplexes formed in water or 50 mM NaCl at a charge ratio (+/−) of 1/1 was significantly decreased. These results clearly indicated that the cellular association of NP-F nanoplexes formed in both water and 50 mM NaCl occurred *via* FR.

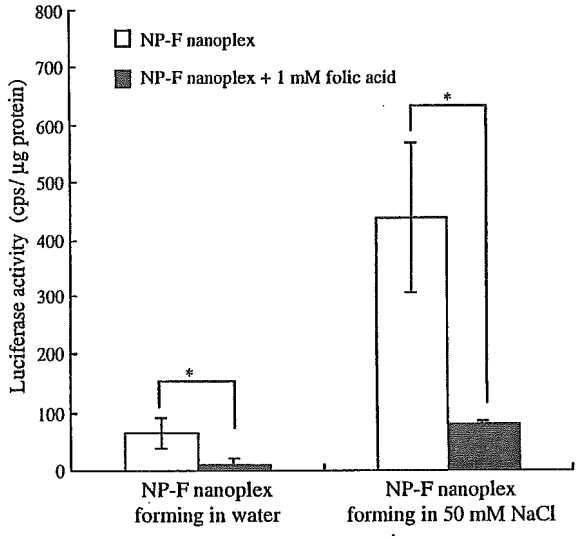

Fig. 9. Luciferase activity in KB cells transfected with NP-F nanoplex for 24 h in the absence or presence of free folic acid. NP-F was mixed with 2 μg of pCMV-luc in water or 50 mM NaCl at a charge ratio (+/−) of 1/1. Each column represents the mean ± SD ($n = 3$). Statistical significance of the data was evaluated by the Welch's t test. $^*P < 0.05$.

4. DISCUSSION

Tissue-targeted gene expression is an important issue regarding safety in gene therapy. Preferential expression of a gene in tumor cells contributes to the safety and the efficacy of gene therapy. The use of cationic cholesterol derivatives could be justified by their high transfection activity and low toxicity.[20] Cationic cholesterol derivatives are composed of three distinct parts: a cholesteryl skeleton, a cationic amino group, and a linker arm between the cholesteryl skeleton and cationic amino group. Derivatives with different combinations of these parts were reported and some of them have high transfection efficiency.[20,21] The cationic cholesterol derivative with a hydroxy amino group, OH-Chol, was reported to have very high transfection efficiency.[10]

Previously, we reported that a folate-linked nanoparticle vector, composed of DC-Chol, Tween 80, and f-PEG_{2000}-DSPE, exhibited selective uptake by KB cells *in vitro*. In this study, we changed the cationic lipid from DC-Chol to OH-Chol in folate-linked nanoparticles (NP-F) and also the nanoplex-forming solution to increase transfection efficiency. The NP-F based on OH-Chol exhibited about 40 times higher transfection efficiency than that based on DC-Chol in KB cells (0.5×10^3 cps/μg protein) (data not shown). It was reported that the hydroxy group of OH-Chol reduced the stability of the lipoplex and enhanced transfection efficiency by facilitating the process by which DNA was liberated from the endosome.[10]

When the amount of f-PEG_{2000}-DSPE in nanoparticles was increased, the association of plasmid DNA with nanoparticles was inhibited significantly (Fig. 1) and a reduction in luciferase activity was observed (Fig. 3A). A large amount of f-PEG_{2000}-DSPE in nanoparticles might prevent enough DNA being carried into the cells and/or reduce the cellular association with the nanoplex as reported in PEG-lipid.[22]

NP-F nanoplex was associated with the cells much more than NP nanoplex after 24 h incubation but induced less luciferase activity (Fig. 3A, B). NP-F nanoplex might be stable on addition of f-PEG_{2000}-DSPE to the NP formula, and plasmid DNA was not efficiently released in the endosome from the nanoplex, resulting in less transfection activity. If the nanoplex is formed in the presence of NaCl, the cationic charge on the surface of the cationic nanoparticles may be neutralized, resulting in the instability of the nanoplex, facilitating the release DNA from nanoparticle and increasing the transfection activity.[19] The transfection activity of nanoplexes formed in various concentrations of NaCl was examined in KB, Hela, and LNCaP cells (Fig. 4A–C). Transfection efficiencies of NP and NP-F nanoplexes formed in increasingly higher concentrations of NaCl were improved. NP-F increased the transfection activity more than NP by forming the nanoplex in 50 mM NaCl solution in KB and LNCaP cells. In contrast to NP-F based on OH-Chol, the nanoparticles based on DC-Chol

RESEARCH ARTICLE

aggregated on the formation of the nanoplex in 50 mM NaCl and did not increase the transfection efficiency (data not shown).

Many parameters including the nanoplex's size are known to affect the transfection efficiency.[11,12] The ionic strength of the nanoplex-forming solution might influence the size and morphology of the particles. In 50 mM NaCl, the NP and NP-F nanoplexes rapidly increased in size (400 and 800 nm, respectively) but did not aggregate for 1 h, while the nanoplex formed in water remained much smaller (Fig. 5). The difference in size between the NP and NP-F nanoplexes formed in 50 mM NaCl solution might be due to the absence or presence of a PEG-chain on the surface of the nanoparticle, because NP-1P nanoplex rapidly increased to almost the same size (800 nm) as NP-F nanoplex in 50 mM NaCl (data not shown). This finding suggested that the effect of NaCl on the transfection of NP-F is likely a result of increased size rather than folic acid linked to NP-F.

Our findings corresponded well with recent studies.[11,12,14,19] PEI/DNA or glucose-grafted PEI/DNA polyplexes formed in NaCl solution led to a higher transfection efficacy into human endothelial cells.[14] In the NaCl solution, the polyplexes rapidly aggregated into large particles (1 μm), while the polyplexes made in 5% glucose remained much smaller (<100 nm). Transfection with the polyplexes prepared in NaCl solution led to a 4- to 25-fold higher level of luciferase gene expression than with those prepared in glucose. Turek et al.[19] reported that large lipoplexes, over 700 nm in mean diameter, prepared in NaCl solution induced efficient transfection, in contrast, lipoplexes of less than 250 nm were inefficient. In our study, to examine the effect of the size of the nanoplex on transfection efficiency, large nanoparticles were prepared by lyophilizing. The lyophilized NP nanoplexes formed in water and NaCl solution increased in size to 540.4 and 808.5 nm, respectively, and increased transfection efficiency 3–4-fold in comparison with unlyophilized NP (280 nm) produced in water (data not shown). The gene transfer efficacy may be highly dependent on the ionic strength of the complex mixing solution. In flow cytometric analysis, the amount of FITC-ODN in KB cells was extensively increased after 3-h incubation (Fig. 6A, B) and in confocal microscopy revealed that FITC-ODN was mostly distributed in the cytoplasm and around the nucleus (Fig. 7B, D, F), using NP and NP-F nanoplexes formed in 50 mM NaCl. The increased uptake of DNA in the cells seemed to correlate with the increased luciferase gene expression (Fig. 4).

Endosome acidification has been well documented in the endocytotic pathway. This suggests that the compartmental pH within cells is lower than that in the growth medium. Most endosomes have pH values between 5 and 6. Therefore, we investigated whether the use of NaCl solution affected the dissociation of DNA from the nanoplex in endosomes. In NP nanoplex, dissociation in buffer of pH 6 and 7 was observed moderately when the nanoplex was formed in water and NaCl solution, respectively (Fig. 8). In contrast, with NP-F nanoplex, little dissociation at pH 6 and 7 was observed when the nanoplex was formed in water (Fig. 8). This might be why NP-F nanoplex could not induce higher transfection efficiency than NP nanoplex when formed in water. However, when NP-F nanoplex was formed in NaCl solution, a marked dissociation of DNA was observed. Thus, nanoplex formation in NaCl solution influenced the size of the nanoplex and extent of DNA dissociation. The reason for the high transfection efficiency of the nanoplex produced in NaCl solution may be its instability, resulting in DNA release in endosomes and the translocation of DNA into the nucleus.

FR-targeted delivery with the NP-F nanoplexes formed in water or NaCl solution was examined in KB cells. NP-F nanoplex formed in 50 mM NaCl solution showed 6.6- and 18.9-fold enhancement of transfection activity with specific receptor association with KB cells, relative to NP-F formed in water at a charge ratio (+/−) of 1/1 and 3/1, respectively (Fig. 4 and 9). Competitive experiments using flow cytometry and luciferase assays revealed that the cellular association and gene expression of neutrally charged NP-F nanoplexes formed in water and NaCl solution at a charge ratio (+/−) of 1/1 was reduced in the presence of free folic acid (Figs. 2 and 9). Furthermore, the amount of FITC-ODN in large positively charged NP-F nanoplexes formed in NaCl solution at a charge ratio (+/−) of 3/1 introduced into the cells after 3-h incubation was increased compared with that of NP (Fig. 6B). These findings suggest that large NP-F nanoplex may restore the interaction between the folate moiety of NP-F and FR of KB cells. The efficient transfection of neutrally charged NP-F nanoplex formed in NaCl solution might be determined mainly by FR-mediated uptake, indicating the usefulness of NP-F as a selective and high transfection vector for cancer cells. The large nanoplexes of NP-F may play an active role in the internalization of DNA into the cells, possibly destabilizing the endosomal vesicles and releasing DNA from the nanoplex into the cytoplasm.

In this study, we showed that folate-linked nanoparticles based on OH-Chol delivered DNA with high transfection efficiency and selectivity into nasopharyngeal KB cells by forming a nanoplex in NaCl solution, which influenced the size of the nanoplex and dissociation of DNA. The results of the experiments have revealed the optimal conditions to form folate-linked nanoparticle complexes with DNA for folate-targeted gene delivery.

Acknowledgments: We thank Mr. Akihiro Hayama for his assistance in our experiment and Dr. Kazuhiro Kubo (NOF Corporation, Tokyo, Japan) for supplying amino-PEG-DSPE. This project was supported in part by a grant from the Promotion and Mutual Aid Corporation for Private Schools of Japan and by a Grant-in-Aid for Scientific

Research from the Ministry of Education, Culture, Sports, Science, and Technology of Japan.

References and Notes

1. C. R. Dass and M. A. Burton, Lipoplexes and tumours. A review. *J. Pharm. Pharmacol.* 51, 755 (1999).
2. I. G. Campbell, T. A. Jones, W. D. Foulkes, and J. Trowsdale, Folate-binding protein is a marker for ovarian cancer. *Cancer Res.* 51, 5329 (1991).
3. M. Wu, W. Gunning, and M. Ratnam, Expression of folate receptor type alpha in relation to cell type, malignancy, and differentiation in ovary, uterus, and cervix. *Cancer Epidemiol. Biomarkers Prev.* 8, 775 (1999).
4. J. F. Ross, P. K. Chaudhuri, and M. Ratnam, Differential regulation of folate receptor isoforms in normal and malignant tissues in vivo and in established cell lines. Physiologic and clinical implications. *Cancer* 73, 2432 (1994).
5. N. Parker, M. J. Turk, E. Westrick, J. D. Lewis, P. S. Low, and C. P. Leamon, Folate receptor expression in carcinomas and normal tissues determined by a quantitative radioligand binding assay. *Anal. Biochem.* 338, 284 (2005).
6. S. M. Stephenson, P. S. Low, and R. J. Lee, Folate receptor-mediated targeting of liposomal drugs to cancer cells. *Methods Enzymol.* 387, 33 (2004).
7. M. A. Gosselin and R. J. Lee, Folate receptor-targeted liposomes as vectors for therapeutic agents. *Biotechnol. Annu. Rev.* 8, 103 (2002).
8. R. J. Lee, and P. S. Low, Folate-mediated tumor cell targeting of liposome-entrapped doxorubicin in vitro. *Biochim. Biophys. Acta* 1233, 134 (1995).
9. G. N. Nabel, E. G. Nabel, Z. Y. Yang, B. A. Fox, G. E. Plautz, X. Gao, L. Huang, S. Shu, D. Gordon, and A. E. Chang, Direct gene transfer with DNA-liposome complexes in melanoma: Expression, biologic activity, and lack of toxicity in humans. *Proc. Natl. Acad. Sci. USA.* 90, 11307 (1993).
10. S. Hasegawa, N. Hirashima, and M. Nakanishi, Comparative study of transfection efficiency of cationic cholesterols mediated by liposomes-based gene delivery. *Bioorg. Med. Chem. Lett.* 12, 1299 (2002).
11. M. R. Almofti, H. Harashima, Y. Shinohara, A. Almofti, W. Li, and H. Kiwada, Lipoplex size determines lipofection efficiency with or without serum. *Mol. Membr. Biol.* 20, 35 (2003).
12. V. Escriou, C. Ciolina, F. Lacroix, G. Byk, D. Scherman, and P. Wils, Cationic lipid-mediated gene transfer: Effect of serum on cellular uptake and intracellular fate of lipopolyamine/DNA complexes. *Biochim. Biophys. Acta* 1368, 276 (1998).
13. E. K. Wasan, P. Harvie, K. Edwards, G. Karlsson, and M. B. Bally, A multi-step lipid mixing assay to model structural changes in cationic lipoplexes used for in vitro transfection. *Biochim. Biophys. Acta* 1461, 27 (1999).
14. V. Zaric, D. Weltin, P. Erbacher, J. S. Remy, J. P. Behr, and D. Stephan, Effective polyethyleneimine-mediated gene transfer into human endothelial cells. *J. Gene Med.* 6, 176 (2004).
15. Y. Hattori and Y. Maitani, Folate-linked nanoparticle-mediated suicide gene therapy in human prostate cancer and nasopharyngeal cancer with herpes simplex virus thymidine kinase. *Cancer Gene Ther.* (2005), in press.
16. Y. Hattori and Y. Maitani, Enhanced in vitro DNA transfection efficiency by novel folate-linked nanoparticles in human prostate cancer and oral cancer. *J. Control Release* 97, 173 (2004).
17. K. Takeuchi, M. Ishihara, C. Kawaura, M. Noji, T. Furuno, and M. Nakanishi, Effect of zeta potential of cationic liposomes containing cationic cholesterol derivatives on gene transfection. *FEBS Lett.* 397, 207 (1996).
18. W. Guo and R. J. Lee, Efficient gene delivery via non-covalent complexes of folic acid and polyethyleneimine. *J. Control Release* 77, 131 (2001).
19. J. Turek, C. Dubertret, G. Jaslin, K. Antonakis, D. Scherman, and B. Pitard, Formulations which increase the size of lipoplexes prevent serum-associated inhibition of transfection. *J. Gene Med.* 2, 32 (2000).
20. R. Okayama, M. Noji, and M. Nakanishi, Cationic cholesterol with a hydroxyethylamino head group promotes significantly liposome-mediated gene transfection. *FEBS Lett.* 408, 232 (1997).
21. A. Percot, D. Briane, R. Coudert, P. Reynier, N. Bouchemal, N. Lievre, E. Hantz, J. L. Salzmann, and A. Cao, A hydroxyethylated cholesterol-based cationic lipid for DNA delivery: Effect of conditioning. *Int. J. Pharm.* 278, 143 (2004).
22. L. Y. Song, Q. F. Ahkong, Q. Rong, Z. Wang, S. Ansell, M. J. Hope, and B. Mui, Characterization of the inhibitory effect of PEG-lipid conjugates on the intracellular delivery of plasmid and antisense DNA mediated by cationic lipid liposomes. *Biochim. Biophys. Acta* 1558, 1 (2002).

Received: 27 January 2005. Revised/Accepted: 14 March 2005.

Available online at www.sciencedirect.com
SCIENCE DIRECT®
ELSEVIER
International Journal of Pharmaceutics 300 (2005) 4–12
international journal of pharmaceutics
www.elsevier.com/locate/ijpharm

Ultra-deformable liposomes containing bleomycin: In vitro stability and toxicity on human cutaneous keratinocyte cell lines

Kent G. Lau [a], Yoshiyuki Hattori [a], Sunil Chopra [b], Edel A. O'Toole [c], Alan Storey [c,d], Tsuneji Nagai [a], Yoshie Maitani [a,*]

[a] *Institute of Medicinal Chemistry, Hoshi University, Ebara 2-4-41, Shinagawa-Ku, Tokyo 142-8501, Japan*
[b] *Department of Dermatology, King George Hospital, Barley Lane, Essex IG3 8YB, UK*
[c] *Centre for Cutaneous Research, Institute of Cell and Molecular Sciences, Barts and the London School of Medicine and Dentistry, Queen Mary, University of London, 2 Newark Street, London E1 2AT, UK*
[d] *Cancer Research UK Skin Tumour Laboratory, Institute of Cell and Molecular Sciences, Barts and the London School of Medicine and Dentistry, Queen Mary, University of London, 2 Newark Street, London E1 2AT, UK*

Received 25 February 2005; received in revised form 4 April 2005; accepted 5 April 2005
Available online 8 June 2005

Abstract

Formulations of ultra-deformable liposomes containing bleomycin (Bleosome™) have previously been described and proposed for topical treatment of skin cancer [Lau, K.G., Chopra, S., Maitani, Y., 2003. Entrapment of bleomycin in ultra-deformable liposomes. S. T. P. Pharm. Sci. 13, 237–239]. In this study, the stability of various Bleosome™ formulations was characterised and a purification process was established to isolate Bleosome™ for testing on cultures of either human cutaneous keratinocytes (NEB-1) immortalised by human papilloma virus (HPV)-type 16, or a spontaneously immortalised human squamous cell carcinoma (SCC) from a primary tumour. Bleosome™ facilitated entrapment of high concentrations of active bleomycin and samples purified by gel-filtration chromatography remained stable during 7 days of storage at 4 °C or at room temperature. Serially-diluted samples of this purified, high-strength product, 'high dose' were applied onto keratinocyte cell cultures to elucidate Bleosome™ LD_{50} profiles.

In vitro data revealed that the LD_{50} of bleomycin encapsulated in Bleosome™ was approximately three-fold higher than free bleomycin solution for SCC cells, and nearly 30 times higher for NEB-1 cells. However, Bleosome™ containing 30 μg/ml of active bleomycin killed more than twice as many SCC cells than NEB-1 cells. At that concentration, the potency of liposomal bleomycin on causing cell death of SCC cells was found to be similar to that of free bleomycin solution. This effect was not seen on NEB-1 cells. It seems that SCC cells were particularly susceptible to Bleosome™ containing high levels of bleomycin. Results from these experiments promote the development of a novel product for the topical treatment of skin cancer.

Keywords: Ultra-deformable liposome; Bleomycin; Keratinocyte cell; Squamous cell carcinoma; Toxicity; In vitro stability

* Corresponding author. Tel.: +81 3 5498 5048; fax: +81 3 5498 5048.
E-mail address: yoshie@hoshi.ac.jp (Y. Maitani).

0378-5173/$ – see front matter © 2005 Elsevier B.V. All rights reserved.
doi:10.1016/j.ijpharm.2005.04.019

1. Introduction

Non-melanoma skin cancer (NMSC) is the most commonly diagnosed cancer in the UK. The incidence of NMSC is rising rapidly and is an important cause of morbidity in the general population and is an increasing burden on healthcare resources.

Ultra-deformable liposomes have shown potential as a carrier for topical drug delivery systems because they can penetrate the skin intact (Cevc et al., 2002). They can be loaded with a wide variety of different therapeutic agents, such as low-molecular weight drugs like 5-fluorouracil (El Maghraby et al., 2001a) as well as larger molecules, such as oestradiol (El Maghraby et al., 2001b), triamcinolone acetonide (Cevc and Blume, 2003), interleukin-2 and interferon-α (Hofer et al., 1999), and even insulin (Cevc et al., 1998) and plasmid DNA (Kim et al., 2004). Bleomycin is an established anti-tumour drug used in the treatment of NMSC. Recent work has shown that bleomycin can be encapsulated in ultra-deformable liposomes and it has been suggested that this preparation may be useful for topical chemotherapy of NMSC (Lau et al., 2003). It is possible to investigate whether encapsulation of bleomycin in ultra-deformable liposomes might alter the lethal potency of this anti-tumour drug by in vitro testing on immortalised, human keratinocyte cell culture model systems. Furthermore, the stability assessment of candidate preparations would provide valuable evidence of which preparations might be viable and suitable for progression to clinical testing.

Several changes to the methodology of the previous study (Lau et al., 2003) have been pursued in these experiments in order to evaluate the possible benefits they might confer. The determination of bleomycin concentration has been conducted with a different solvent system and ion-pairing agent (Fiedler and Wachter, 1991, cf. Aszalos et al., 1981) that dramatically reduces the duration required to analyse each sample, thus allowing higher throughput and rapid monitoring of Bleosome™ preparations. Gel-filtration chromatography was used in this study to isolate and purify Bleosome™ preparations for keratinocyte toxicity studies. This technique is less invasive than ultra-centrifugation and would avoid the possibility of irreversible compaction and aggregation of Bleosome™. Nonetheless, ultra-centrifugation was still a suitable isolation technique in the course of determining bleomycin concentration in Bleosome™ because liposomal integrity would ultimately be breached by addition of methanol in order to release the drug for assaying.

It was essential to test Bleosome™ preparations on human cell types similar to the targeted diseased tissue because the response of human keratinocytes to drug treatment may be dissimilar from that of keratinocytes from murine or other animal sources. Cell cultures of human papilloma virus (HPV)-type 16 immortalised human keratinocytes (NEB-1) were used as a model for an immortalised human keratinocyte cell line that is not tumourigenic in nude mice (Morley et al., 2003). Cell cultures of spontaneously immortalised human squamous cell carcinoma (SCC) were grown from primary lesions (Purdie et al., 1993) and utilised as a model of human SCC. These two types of keratinocytes formed the basis of initial testing of Bleosome™ toxicity in vitro and calculation of LD_{50} responses. Potency of Bleosome™ could then be compared against the toxic profiles of free bleomycin solution at an equivalent concentration.

The aim of this study was to evaluate the in vitro bioefficacy of Bleosome™ on immortalised and malignant human keratinocytes. Another objective was to assess the physical stability of such preparations in vitro, with regards to particle size and bleomycin retention. The results from these experiments will facilitate development of a clinical preparation suitable for testing on human subjects.

2. Materials and methods

2.1. Materials

Bleomycin hydrochloride for injection was purchased from Nippon Kayaku Co. (Tokyo, Japan). Egg phosphatidycholine (ePC) was purchased from Avanti Polar Lipids (Alabaster, AL). Sodium cholate was obtained from Sigma Chemicals (St. Louis, MO). Sodium perchlorate and other chemicals used were of reagent grade and purchased from Wako Pure Chemical Industries Ltd. (Osaka, Japan).

2.2. Preparation of ultra-deformable, multi-lamellar liposomes containing bleomycin

Multi-lamellar liposomes (MLVs) were prepared using a modified, dry-film method. Briefly, formu-

lations of ePC, with (5, 10 or 16%, w/w) or without sodium cholate, were dissolved in ethanol, which was removed by rotary evaporation, in a nitrogen atmosphere. The dry-lipid film was hydrated with 10% (w/v) bleomycin hydrochloride solution and diluted with the appropriate strength of phosphate-buffered saline (PBS, pH 7.4) to yield a liposomal suspension of 1% bleomycin hydrochloride for a preliminary stability test, and with 1/10-diluted PBS (1/10 PBS) to yield 'low' dose Bleosome™ for cytotoxicity test. Final lipid concentration was 0.1 mM. The 'high' dose Bleosome™ was prepared by purification of by gel chromatography described in Section 2.5.

2.3. Determination of bleomycin entrapment efficiency

Bleomycin MLV suspensions were centrifuged at 100,000 × *g* for 360 min to separate the free bleomycin in the supernatant from the liposomal bleomycin. Upon removal, the liposome pellet was dissolved using methanol and the amount of active bleomycin congeners A2 and B2, and inactive A2 in 10 μl of the supernatant or pellet was determined by ion-pair high-performance liquid chromatography (HPLC), 717 plus autosampler, 600S controller, 616 pump (Waters; MA, USA) and UV detector at 240 nm (L-4000, Hitachi, Tokyo, Japan) with sodium perchlorate. Based on a method by Fiedler and Wachter (1991), a 5% (v/v) acetonitrile in 0.1 M phosphoric acid and 10 mM sodium perchlorate, pH 4.3 was increased to 25% (v/v) with line gradient over 20 min and then increased to 100% for 2 min and hold for a 2 min at room temperature and at a rate of 1 ml/min through a C_{18} (ODS) column (TSK-GEL, Tosoh, Tokyo, Japan) of 25 cm × 4.6 mm. The first two primary peaks represent active bleomycin A2 and B2, respectively, and the third major peak relates to inactive bleomycin A2 (Fig. 1). A calibration curve was produced using commercial bleomycin in the range of 1–1000 μg/ml.

2.4. Particle size and zeta-potential measurements

The average diameters of MLV vesicles were determined by dynamic light scattering using a laser light-scattering instrument (ELS 800, Otsuka Electronics Co. Ltd., Osaka, Japan). The samples were diluted in distilled water in order to avoid multiple scattering. The measurements were performed at 25 ± 0.1 °C, at an angle of 90° between laser and detector.

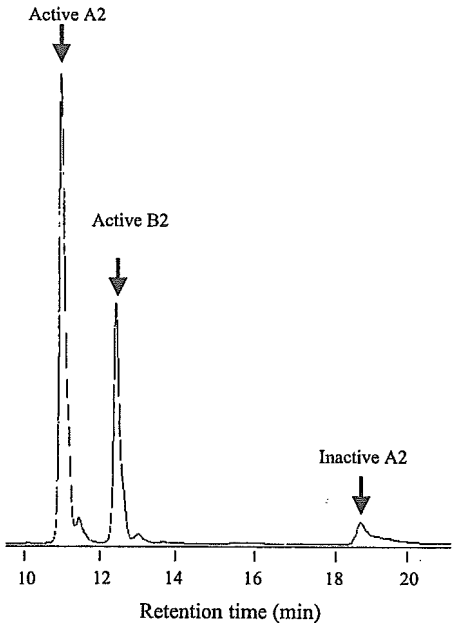

Fig. 1. High-performance liquid chromatography (HPLC) separation of a commercial sample of bleomycin hydrochloride revealing three major peaks: active bleomycin A2 (time = 10.9 min); active bleomycin B2 (time = 12.3 min) and inactive demethyl-bleomycin A2 (time = 18.6 min).

2.5. Liposome purification

Bleosome™ containing bleomycin was separated from free bleomycin by gel-filtration chromatography. A column of Sephadex G-50 was prepared in a burette (25 cm × 1 cm) and equilibrated with 1/10 PBS. Eluent fractions of 1 ml/min were collected for 50 min. A UV-spectrophotometric trace revealed which fractions contained the highest concentrations of Bleosome™. The most concentrated three fractions (each fraction 1 ml) were pooled to form a stock suspension for testing on keratinocytes.

2.6. Stability study

A preliminary study of individual Bleosome™ preparations in PBS was evaluated at two different

temperatures (room temperature at 25 °C and refrigerated at 4 °C) for 8 days. Samples were taken daily for analysis, as noted in Sections 2.3 and 2.4 above. Subsequent studies were only carried out on the preferred candidate preparation (10% (w/w) sodium cholate), which was kept in 1/10 PBS, at room temperature (25 °C), and sampled daily for 7 days. Due to batch-to-batch variation, it was necessary to monitor the stability of the actual preparation that was used for the keratinocyte toxicity tests.

2.7. Cell culture

Two types of keratinocytes were tested with 'high' (1091.5 ± 25.8 μg/ml active bleomycin; $n=3$) and 'low' (22.3 ± 8.2 μg/ml active bleomycin; $n=3$) dose Bleosome™. Firstly, NEB-1 cells were cultured and used as a model for human papilloma virus (HPV)-associated disease. Secondly, SCC cells were grown and used as a model for NMSC in general. These cell lines were maintained in standard keratinocyte tissue culture medium: Dulbecco's modified Eagle's medium with 25% Ham's F12 medium, 10% fetal calf serum, 10 ng/ml epidermal growth factor, 0.4 μg/ml hydrocortisone, 10^{-10} mol/l cholera toxin, 5 μg/ml transferrin, 2×10^{-11} mol/l lyothyronine, 1.9×10^{-4} mol/l adenine and 5 μg/ml insulin, supplemented with 3T3 fibroblast feeder cells (Morley et al., 2003). Cells that remained alive after 2 days exposure to Bleosome™ or bleomycin solution were counted using WST-8 reagent solution (Dojindo, Kumamoto, Japan) and a UV-spectrophotometer.

3. Results

3.1. Stability studies

The quantity of sodium cholate in each 'low dose' Bleosome™ formulation had an effect on bleomycin entrapment levels and average particle size (Figs. 2 and 3), but refrigeration at 4 °C over a time period of 8 days did not improve liposome stability when compared to similar samples stored at room temperature. Control liposomes without sodium cholate exhibited the largest size and the lowest capacity for bleomycin entrapment, whereas liposomes featuring 16% sodium cholate yielded the smallest size, but their capability for entrapping bleomycin was still relatively poor. Although liposomes containing 5 or 10% sodium cholate exhibited similar tendencies with respect to size and bleomycin entrapment, in the absence of further refinement, it was considered that Bleosome™ preparations featuring 10% sodium cholate merited selection for further study since they encapsulated the most bleomycin.

It had been noted that the average particle size of the various Bleosome™ preparations incorporating sodium cholate was significantly larger than the data seen in a previous study (Lau et al., 2003). This was thought to be a result of storage in PBS and the possible occurrence of ion–charge interactions that increased the inter-lamellar distance, and consequently caused an expansion within liposome particles. In order to avoid this effect, thereafter, Bleosome™ preparations were stored in 1/10 PBS and their average particle

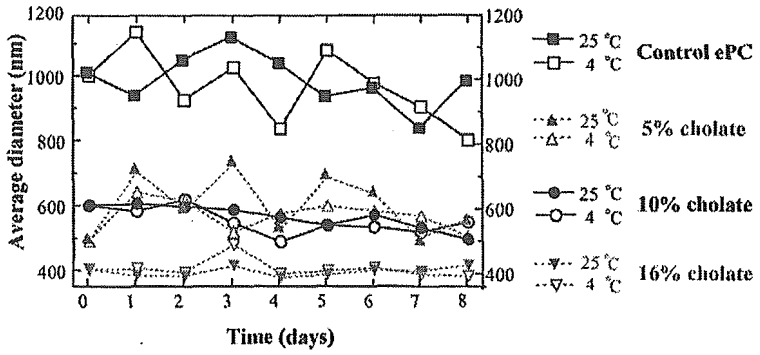

Fig. 2. Comparing average particle size (nm) of 'low dose' Bleosome™ formulations incorporating various concentrations of sodium cholate against control liposomes without any sodium cholate, whilst being stored in PBS, at refrigerated (4 °C) and room temperatures (25 °C) over 8 days ($n=1$).